Sensors & Diagnostics

PAPER

View Article Online
View Journal | View Issue

Cite this: *Sens. Diagn.*, 2022, **1**, 516

Highly crystalline N and S co-doped carbon dots as a selective turn off–on sensor for Cr(VI) and ascorbic acid and a turn off sensor for metanil yellow†

Ambreen Abbasi and Mohammad Shakir *

Highly crystalline N and S co-doped carbon dots (NS CDs) were synthesized by a hydrothermal method using mesaconic acid, ethylenediamine, and sulfuric acid as C, N, and S sources. The prepared NS CDs displayed blue fluorescence emission (λ_{ex} = 350 nm and λ_{em} = 405 nm) and exhibited a high quantum yield of 33%. The synthesized NS CDs were spherical and had a mean particle diameter of 3.5 ± 0.86 nm. The prepared carbon dots have large functional groups on their surface, which makes them have excellent water solubility. NS CDs were used as a selective and sensitive turn off and turn on sensor for detection of Cr(VI) with a linear response ranging from 3 μM to 60 μM with a detection limit of 0.056 μM and ascorbic acid with a linear response ranging from 3 μM to 126 μM with a detection limit of 1 μM. The NS CDs also served as a selective and sensitive turn-off sensor for metanil yellow with a linear response ranging from 3 μM to 130 μM with a detection limit of 0.14 μM. The Cr(VI) recognition mechanism was suggested to be a combination of static quenching and the inner filter effect. At the same time, for the detection of ascorbic acid and metanil yellow, it was proposed to be the inner filter effect. The actual sample application of NS CDs as a nanosensor was studied for detection of metanil yellow as an adulterant in turmeric powder.

Received 3rd November 2021,
Accepted 12th March 2022

DOI: 10.1039/d1sd00042j

rsc.li/sensors

1. Introduction

During the past decade, carbon dots have appeared as a new luminescent material.[1] They have drawn extensive attention as they have numerous beneficial features such as chemical stability, outstanding photostability, low toxicity, high fluorescence quantum yield, and ease of surface fabrications,[2] which have led to their widespread applications in fluorescence sensing and bioimaging and as a photocatalyst, in energy storage and conversion, optoelectronic devices, drug delivery, and printing ink,[3] and a fluorescent probe for biomedical application and environmental remediation.[4] In recent years, researchers have focused on doping carbon dots with heteroatoms to improve their fluorescence efficiency and sensing selectivity.[5] Among the various non-metals used as dopants for carbon dots, nitrogen doping has gained tremendous interest as the electrons trapped in the new-formed N-state can exhibit high fluorescence yield.[6]

The electronic structure of carbon dots can be optimized by doping with sulfur. The addition of sulfur could provide the density of states or create emissive trap states for photoexcited electrons, modifying the bandgap energy.[7] The introduction of sulfur can eliminate the O states and could enhance the N states.[6] In other words, the effects induced by nitrogen in N-CDs can be enhanced by the introduction of sulfur *via* a cooperative effect.[8] Ping Ni *et al.* have reported nitrogen and sulfur co-doped carbon dots synthesized from cysteine as a precursor with a quantum yield of 38% and have demonstrated their applicability as fluorescent probes for living cell imaging.[9] Qianghua Ye *et al.* have reported the formation of N and S co-doped CDs from biomass with a quantum yield of 24.8%. They have used the synthesized CDs for selective detection of mercury and iron ions.[10] Chen J. *et al.* have prepared nitrogen and sulfur co-doped carbon dots *via* hydrothermal synthesis using citric acid and cystamine dihydrochloride precursors with a quantum yield of 39.7%. They have used the synthesized carbon dots for detection of Cr(VI) ions *via* the inner filter effect.[11] Eliana F. C. Simões *et al.* have reported N and S co-doped carbon dots as a selective sensor for nitric oxide.[12] Shouming Xu *et al.* have

Division of Inorganic Chemistry, Department of Chemistry, Aligarh Muslim University, Aligarh 202002, India. E-mail: shakir078@yahoo.com; Tel: +919837430035

† Electronic supplementary information (ESI) available. See DOI: 10.1039/d1sd00042j

synthesized N and S co-doped carbon dots from casein with a quantum yield of 31.8% for sensitive detection of Hg^{2+}.[13]

Due to the amorphous nature of most well-documented carbon dots, it isn't easy to have a generalized idea about their properties and thus application potential.[14] Therefore, it is highly desirable to introduce crystallinity into carbon dots to improve their application potential, especially in high-efficiency electron and energy transfer.[15]

Hexavalent Cr(VI) has been reported to pose a more significant threat to human health because of its high toxicity, water-solubility, carcinogenesis, teratogenicity, and mutagenicity.[16] Even though the World Health Organization (WHO) has set a consumption limit of 0.05 μg ml^{-1} for Cr(VI), there is still a lack of studies to figure out the minimum amount of Cr(VI), which could lead to disease when ingested.[17] Zhang H. *et al.*, Laddha H. *et al.*, and Anand S. R. *et al.* have all reported N and S co-doped carbon dots as a selective sensor for Cr(VI) ions.[18–20]

Ascorbic acid, commonly known as vitamin C, plays a vital role in maintaining healthy physiological functions.[21] However, as it is known that the human body cannot synthesize ascorbic acid, it has been acquired from food, and drugs.[22] The deficiency of ascorbic acid has been related to many diseases such as cancer, cardiovascular diseases, and Parkinson's disease.[23] However, numerous methods for detecting ascorbic acid have been reported in the literature, such as HPLC,[24] UV-vis spectroscopy,[25] electrochemical processes[26] and fluorescence methods.[27–30] Amongst all methods, fluorescence methods are highly desirable because of their high sensitivity, high selectivity, simplicity, and convenience.[31]

Metanil yellow is a banned toxic azo dye, which has been added to turmeric powder to mimic the appearance of curcumin.[32] Metanil yellow has been cited in the literature to cause testicular damage in guinea pigs, rats, and mice; it is reported to induce hematological changes and affect the synthesis of DNA.[33] Therefore, the need to detect metanil yellow in food is of paramount importance.

This paper reports the synthesis, characterization, and sensing application of highly crystalline nitrogen and sulfur co-doped carbon dots. The attractive feature of our nanosensor is that it exhibits highly ordered non-graphitic polycrystallinity; such crystallinity in carbon dots is rare as most of the reported carbon dots are either amorphous or they exhibit graphitic crystallinity. Also, mesaconic acid as a carbon source for synthesizing carbon dots is not reported in the literature. The present NS CDs also exhibit a stable fluorescence response in a wide pH range, which is also uncommon as the fluorescence of most of the reported carbon dots is pH-dependent. Our synthesized nanosensor serves as a single sensor for detecting multiple analytes with good sensitivity, selectivity, and fast response time. To the best of our knowledge, not much work for the fluorescence sensing of metanil yellow using nitrogen sulfur-doped carbon dots is reported in the literature. Further, our advanced sensor could be used for practical applications.

2. Experimental

See the ESI.†

3. Results and discussion

3.1. Characterisation of the NS CD sensor

The TEM image shown in Fig. 1a affirms the spherical shape of the reported carbon dots. The size distribution histogram (inset of Fig. 1a) shows that the size distribution of CDs is from 1.5 nm to 5.5 nm with a mean particle diameter of 3.5 ± 0.86 nm, which was evaluated by counting 84 particles. The sharp patterns in the SAED image (Fig. 1b) and several distinct fringes in the IFFT patterns (Fig. 1c and d) with a lattice spacing of 0.12 nm, 0.17 nm, 0.21 nm, and 0.34 nm reveal the highly polycrystalline nature of the synthesized NS CDs. The lattice spacing of 0.17 nm and 0.21 nm in the present study corresponds to the crystallinity in the carbon nanostructure itself.[15]

Powder X-ray diffraction analysis results further supported this polycrystalline nature of the NS CDs. The diffraction pattern of the NS CDs (Fig. 2) consisted of remarkably well-defined sharp peaks at 2θ values of 15.56°, 19.76°, 20.9°, 21.5°, 23.24°, 28.29°, 29.84°, and 31.46°. Such well-defined peaks have been reported in the literature for similar highly ordered polycrystalline non-graphitic carbon dots.[15,34]

Fig. S1† shows the absorption spectrum of the NS CDs. Like earlier reported CDs, the NS CDs mainly exhibit absorption in the UV region with a tail extending to the whole visible region.[11] The peaks in their absorption spectrum are mainly centered at 289 nm and 330 nm, respectively, belonging to the π–π* transition of the C═C bond and the n–π* transition of the C═O bond.[35] The aqueous NS CDs exhibited light yellow color in daylight and bright blue fluorescence when illuminated with 365 nm UV light (inset of Fig. S1†). The emission spectra of the NS CDs at different excitation wavelengths are shown in Fig. S2.† It is shown that the NS CDs exhibited a wavelength-dependent behavior. However, the emission wavelength remained almost unchanged when excited from 280 to 350 nm with an increase in the intensity, and thereupon the emission wavelength red-shifted from an excitation wavelength of 360 to 420 nm. The maximum emission intensity was observed at 405 nm with an excitation wavelength of 350 nm; so these excitation and emission wavelengths were used throughout the study. The diverseness of the functional groups on the CD surface has been reported in the literature to cause a bathochromic shift of emission wavelength on increasing the excitation wavelength[36] by generating intervening states between the LUMO and HOMO orbitals of CDs, thus permitting emission over a more excellent range of the electromagnetic spectrum.[36] The quantum yield of NS CDs was found to be 33% (Table S1†).

In comparison, NCDs synthesized without adding sulphuric acid have a quantum yield of 13.8% (Table S2†). Efforts to isolate the NCDs failed because of the formation of

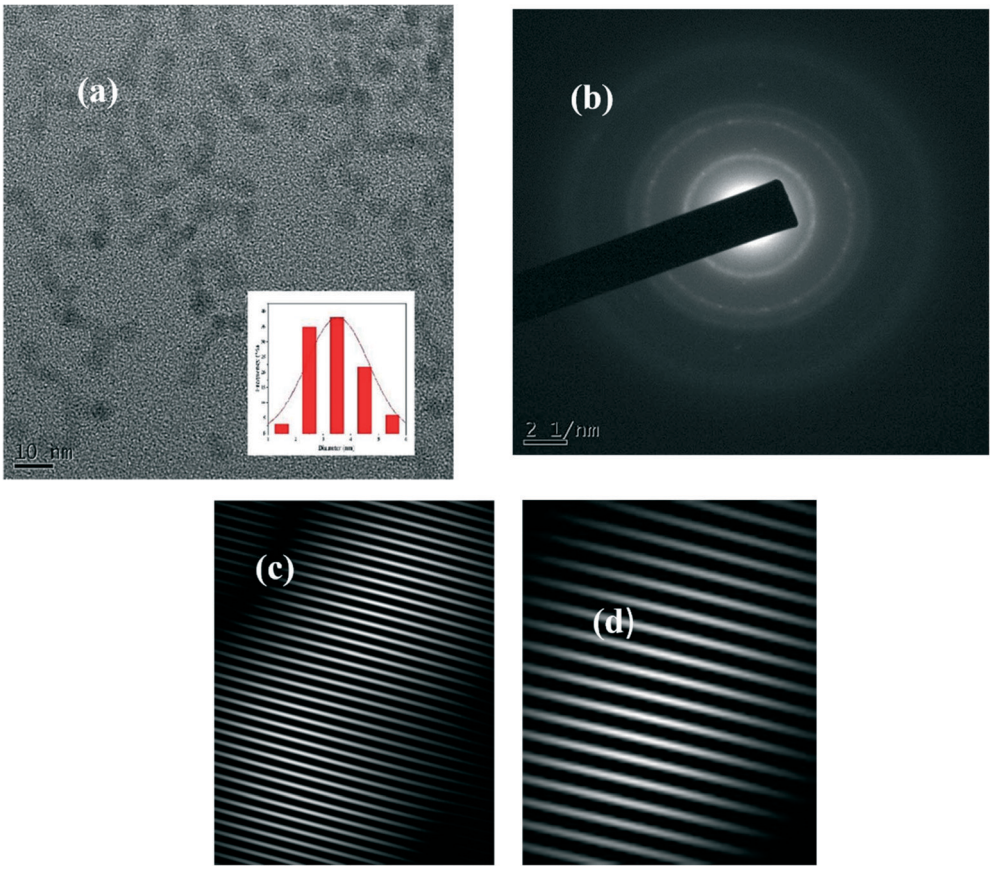

Fig. 1 (a) TEM image of the NS CDs, (b) SAED image, and (c and d) IFFT patterns.

sticky mass after drying. The fluorescence behaviour of NCDs was also different from the NS CDs. The maximum excitation and emission wavelengths of the NCDs was 320 nm and 380 nm. Also, enhancement in the fluorescence intensity for the NS CDs is observed in Fig. S3.† Therefore, the NS CDs were used as a nanosensor for our study. No carbon dots were formed using mesaconic acid alone and mesaconic acid and sulphuric acid.

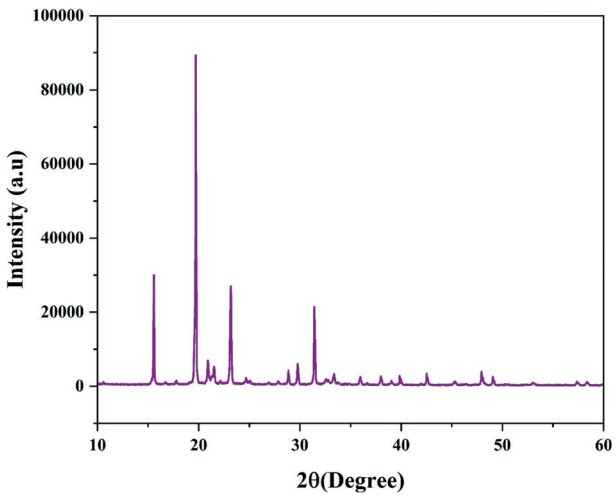

Fig. 2 XRD pattern of the NS CDs.

An FT-IR study was carried out to get a better insight into the various functional groups attached to the surface of carbon dots. The broadband in Fig. 3 between 3000 and 3500 cm^{-1} provides evidence for the presence of the O–H or N–H bond stretching vibration.[37] The band at 1398 cm^{-1} is ascribed to the N–H stretching vibration in the amide bond. The stretching vibrations of N–H in amine salts are found at 2598 cm^{-1}, 2488 cm^{-1}, and 2374 cm^{-1}.[38] The carbonyl stretching vibration in the carboxylic functional group is found at 1700 cm^{-1} (ref. 39), while that in the amide bond is seen at 1680 cm^{-1}. The N–H bending vibration in secondary amides is found at 1542 cm^{-1}, while the O–H and C–O/C–N bending vibrations are seen at 1348 cm^{-1} and 1100 cm^{-1}, respectively. The ═C–H bending vibration is attributed to the band at 988 cm^{-1}. The peaks corresponding to SO_3^{2-}/SO_4^{2-} are at 640 cm^{-1} and 613 cm^{-1}.[38]

These results supported that the synthesized CDs were successfully doped with N and S, which was further backed by the EDS spectrum results (Fig. S4†), which clearly showed the peaks of the N and S atoms. The elemental composition of NS CDs was elucidated further with an elemental analyzer showing 40.38% C, 5.97% H, 10.659% N, 10.539% S, and 32.45% O (calculated). The TGA spectrum (Fig. S5†) of the NS CDs shows a minor weight loss up to 250 °C due to the removal of the attached water molecules on the surface of the CDs; thereupon, the weight loss up to 800 °C has been ascribed to continuous degradation of the CDs.

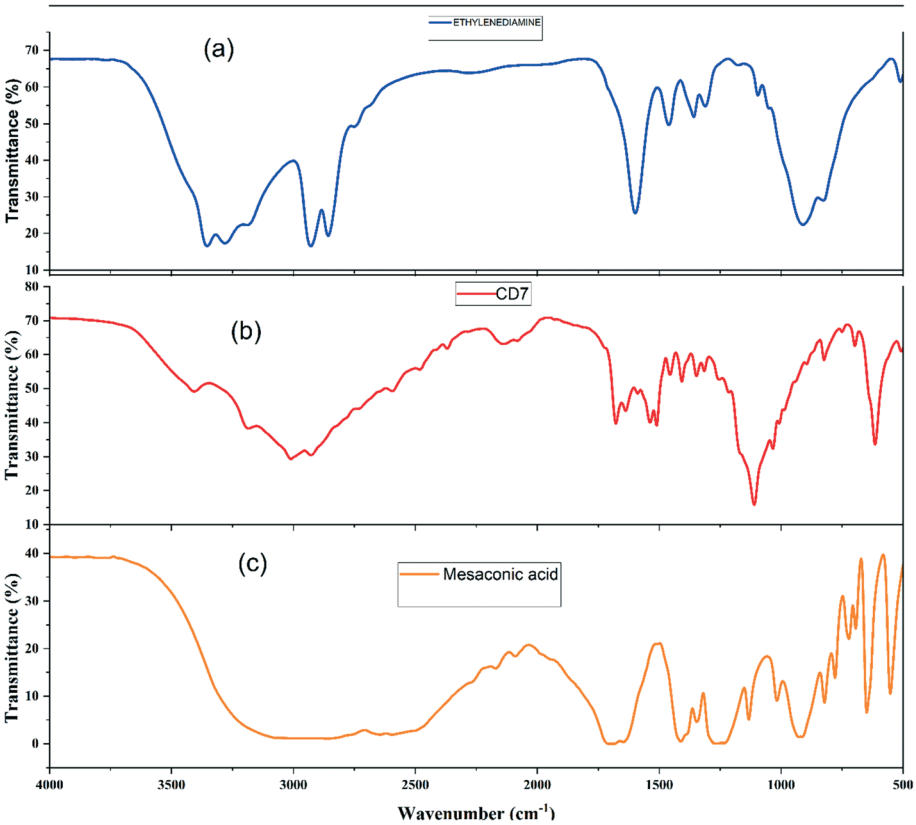

Fig. 3 IR spectra of (a) ethylenediamine, (b) the NS CDs, and (c) mesaconic acid.

3.2. The fluorescence stability of the NS CDs

The fluorescence intensity of the NS CDs under different pH conditions was studied. As shown in Fig. S6,† the fluorescence intensity of the prepared CDs did not show much variation in the wide pH range from 2–11, thereby signifying their potential applications in the wide pH range compared to other reported carbon dots. Such high stability in the fluorescence intensity over a wide pH range can be due to the presence of many C═O and OH groups instead of easily ionizable NH_2 and COOH groups.[40] From this observation, it can be proposed that the surface states responsible for the fluorescence of the NS CDs were not much affected with the variation of pH from acidic to alkaline. However, as depicted in Fig. S7,† the fluorescence intensity of the prepared NS CDs remained unchanged for 160 min after exposure to xenon arc light, suggesting their agreeable photostability. The effect of increasing ionic strength on the fluorescence intensity of the NS CDs was investigated by adding 0 to 0.5 M NaCl into the NS CD solution. Fig. S8† displays that the intensity of the NS CDs is not showing much variation indicating the excellent optical stability of these CDs under a high ionic strength.

3.3. Sensitive and selective recognition of Cr(VI) by the NS CDs

As shown in Fig. S9,† the maximum quenching of the fluorescence intensity on the addition of Cr(VI) was observed at pH 7; so this pH was chosen for the entire study. The reason for this behaviour has been cited in the literature as the greater molar volume of dichromate, which is the predominant form of Cr(VI) in the acidic medium, than chromate, which makes dichromate have lower electron density as compared to chromate, which is further responsible for its less effective interaction with CDs at lower pH.[41] Further, the alkaline conditions lead to deprotonation of oxygen-containing groups, thereby enhancing the negative charge on the surface of the CDs, thus disfavouring the interaction of the CDs with negatively charged chromate ions; this resulted in decreased quenching efficiency under alkaline conditions.[10] Moreover, as shown in Fig. S10,† on the addition of 50 μM of Cr(VI) to the NS CD solution, the fluorescence intensity of the CDs was quenched within a minute.

To investigate the effect of the increasing Cr(VI) concentration on the fluorescence intensity of the NS CDs, fluorescence titration experiments were carried out at 350 nm excitation and 405 nm emission wavelengths. As shown in Fig. 4a, with an increase in the Cr(VI) concentration from 0 to 150 μM, the fluorescence intensity of the NS CDs gradually decreased with a 20 nm red shift in the emission wavelength. Blue fluorescence disappeared on the gradual addition of Cr(VI) (inset of Fig. 4a). Excellent linearity for the Cr(VI) concentration is exhibited in the concentration range 3 to 60 μM (Fig. 4b). The LOD was calculated to be 0.056 μM. The

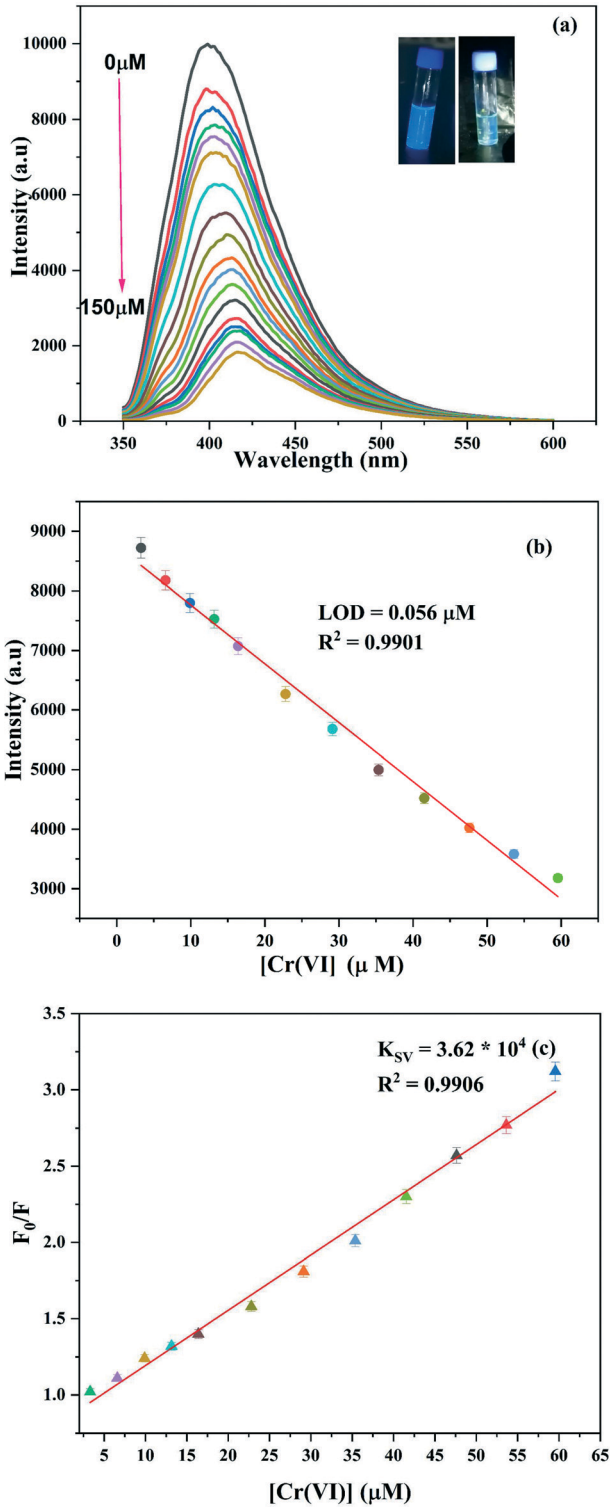

Fig. 4 (a) Change in the fluorescence intensity of the NS CDs with the increase in the concentration of Cr(VI). (b) Calibration curve for the LOD. (c) Stern–Volmer plot of Cr(VI).

following equations were used to calculate the Stern–Volmer (K_{SV}) constant

$$F_0/F = 1 + K_{SV}[\mathrm{Cr(VI)}] \text{ or } F_0/F = 1 + K_q\tau_0[\mathrm{Cr(VI)}]$$

where F_o and F are fluorescence intensities of NS CDs in the absence and presence of Cr(VI), respectively, and K_{SV} is the Stern–Volmer quenching constant, which was found to be 3.62×10^4 L mol^{-1} from the slope of the plot of F_0/F *vs.* [Cr(VI)] (Fig. 4c). K_q is the bimolecular quenching rate constant, τ_0 is the average lifetime of NS CDs in the absence of Cr(VI). The present method was compared to the most sensitive approaches previously reported (Table S3†).

The selectivity of the synthesized NS CD sensor towards Cr(VI) was investigated against 20 metal ions. As can be inferred from Fig. S11,† only Cr(VI) was able to quench the fluorescence intensity of the CDs at a concentration of 150 μM against the concentration of other metal ions, which were taken to be ten times that of Cr(VI) concentration, thus demonstrating the high selectivity of the sensor towards Cr(VI). The interference of other ions on the Cr(VI)'s quenching response was also explored. Fig. S12† shows that most of the studied ions have no impact on the quenching response of Cr(VI) except for Pb(II) and Ba(II), both of which led to further quenching of the emission intensity of the NS CDs + Cr(VI) solution. The probable reason for the interference of these ions could be that these ions are known to form low solubility salts with chromate ions.

3.4. Sensitive and selective detection of ascorbic acid

The turn-off response of Cr(VI) towards NS CD fluorescence intensity was restored by adding ascorbic acid. As shown in Fig. S12,† amongst the various tested reducing agents, only ascorbic acid was successful in restoring the fluorescence of the NS CDs. The turn-on response of ascorbic acid towards the NS CDs + Cr(VI) ensemble was completed within 2 minutes and remained stable for one hour (Fig. S10†). On gradual addition of ascorbic acid to the NS CDs + Cr(VI) mixture solution, the fluorescence intensity showed enhancement with a 20 nm blue shift (Fig. 5). Blue

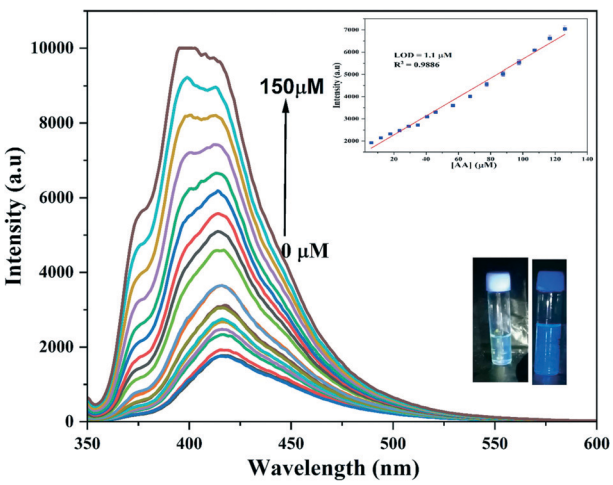

Fig. 5 Change in the fluorescence intensity of NS CDs-Cr(VI) on the addition of ascorbic acid. The insets show the calibration curve for the LOD and restoration of the fluorescence intensity on addition of ascorbic acid.

fluorescence emission under 365 nm UV light was also seen to be restored on the addition of ascorbic acid (inset of Fig. 5). The linear relationship between the concentration of ascorbic acid and fluorescence intensity was found in the 3 μM to 126 μM range. The LOD was calculated to be 1 μM (inset of Fig. 5).

3.5. Sensitive and selective detection of metanil yellow

As shown in Fig. S14,† the quenching of the fluorescence intensity on the addition of metanil yellow was almost constant in the studied pH range, with slightly more quenching at pH 7; so this pH was chosen for the study. As shown in Fig. S15,† metanil yellow successfully quenched the fluorescence of the NS CDs amongst the various tested dyes. The turn-off response of metanil yellow towards the NS CDs was completed within a minute and remained stable for one hour (Fig. S16†). The fluorescence intensity was quenched on gradually adding metanil yellow to the NS CD solution (Fig. 6a). The linear relationship between the concentration of metanil yellow and the fluorescence intensity was found in the 3 μM to 130 μM range (Fig. 6b). The LOD was calculated to be 0.14 μM. K_{SV} was found to be 8.34×10^3 L mol^{-1} from the slope of the plot of F_0/F *vs.* [MY] (Fig. 6c). The present method is compared to different approaches reported for the detection of metanil yellow (Table S4†).

3.6. Mechanism of Cr(VI), ascorbic acid, and metanil yellow sensing by the NS CDs

3.6.1. Mechanism of Cr(VI) and ascorbic acid sensing by the NS CDs. Fig. S17 and S18† show the UV-vis spectrum of Cr(VI) and the excitation and emission spectra of the NS CDs and NCDs. As can be seen, there is an appreciable overlap between the absorption bands of Cr(VI) and the excitation and emission spectra of the NS CDs. At the same time, Cr(VI) can only screen emitted light for NCDs. Such a spectral overlap signifies that Cr(VI) is capable of screening excited as well as emitted light of the NS CDs leading to the effective inner filtration effect between CDs and Cr(VI) and consequently causing increased quenching of the fluorescence intensity of the NS CDs in the presence of Cr(VI)[42,43] as compared to the quenching of the fluorescence intensity of the NCDs. Fig. S19† shows a comparison of NCDs and NS CDs with Cr(VI) to study the influence of N and S doping for sensing Cr(VI). As shown in Fig. 4a, there was an apparent red-shift of 20 nm in the emission wavelength on the addition of Cr(VI), thus implying that the inner filter effect alone is not responsible for fluorescence quenching. To get an insight on what other factor is playing a role in the detection process, the absorption spectrum of the NS CDs was studied in the presence of Cr(VI). As shown in Fig. S20† on the addition of 10 μM of Cr(VI) to the NS CD solution, the absorption bands of the NS CDs shifted to 284 nm and 344 nm from 289 nm and 330 nm, and on increasing the concentration of Cr(VI), the 284 nm band blue-shifted to 262 nm, and the 330 nm band red-shifted to 360 nm, signifying some interactions between CDs and Cr(VI), indicative of the probability that the quenching mechanism is static.

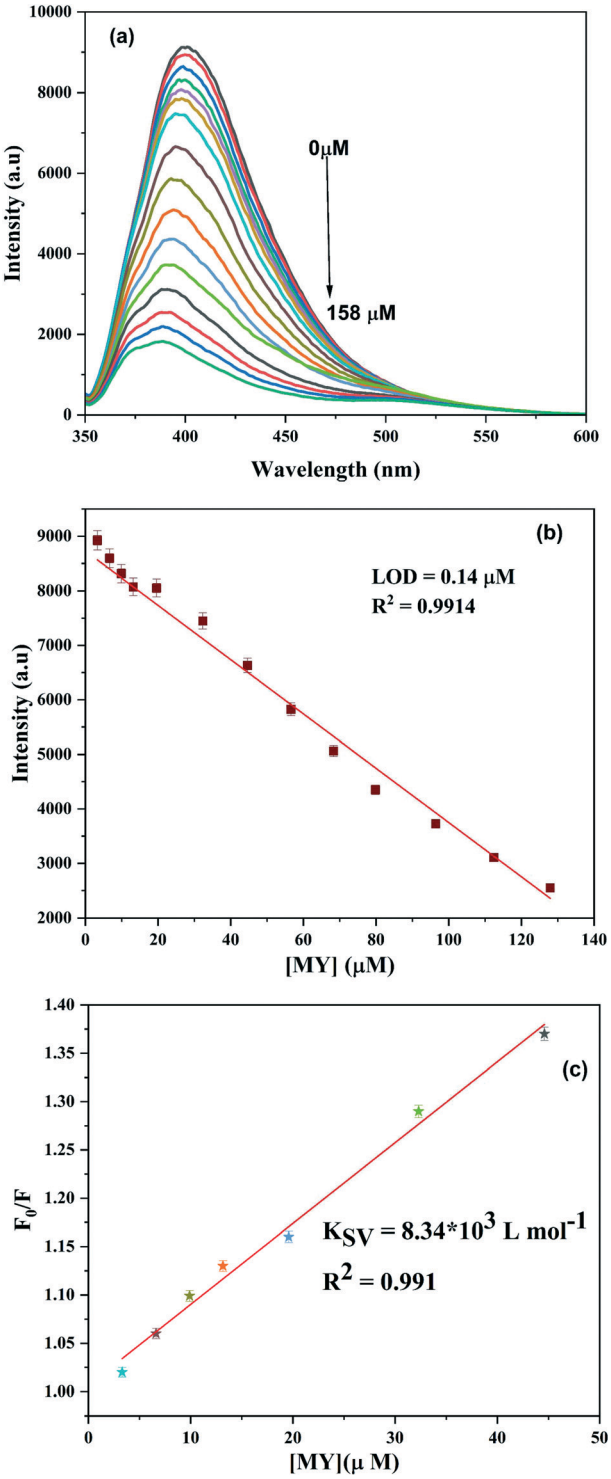

Fig. 6 (a) Change in the fluorescence intensity of the NS CDs on the addition of metanil yellow. (b) Calibration curve for the LOD. (c) Stern–Volmer plot.

Further, this absorption spectrum of NS CDs-Cr(VI) may further be masking NS CDs' excitation radiation, leading to a decrease in the fluorescence intensity. Such a change in the

absorption spectrum of the NCDs was not seen: the absorption band of the NCDs showed no change in position, and on addition of Cr(VI), no new band was formed, and only the band of Cr(VI) was seen at their expected position (Fig. S21†). The K_q value further supported the interaction between the NS CDs and Cr(VI), 1.096×10^{13} L mol^{-1} s^{-1}. The literature reported that the value of K_q is less than 2×10^{10} L mol^{-1} s^{-1} for dynamic quenching, while the higher values suggest static quenching.[44] Such interactions between CDs and Cr(VI) have been reported in the literature.[45,46] However, the fluorescence decay profile of the NS CDs in the absence and presence of Cr(VI) did not change. The lifetime remained almost the same in Cr(VI) (Table S5, Fig. S22†).

As shown in Fig. S23,† the absorbance of NS CDs-Cr(VI) at 360 nm disappeared on gradual addition of ascorbic acid because of the greater affinity of ascorbic acid towards Cr(VI). The addition of ascorbic acid to the NS CDs-Cr(VI) mixture resulted in the reduction of Cr(VI) to Cr(III), which led to the elimination of the inner filter effect resulting in the restoration of the fluorescence intensity of the NS CDs.

3.6.2. Mechanism of metanil yellow sensing by the NS CDs. As shown in Fig. S24,† the absorption spectrum of metanil yellow exhibited bands at 273 nm and 438 nm, which is showing a good spectral overlap with the excitation and emission spectra of the NS CD sensor resulting in metanil yellow's effective screening of both the excitation and emission radiation of the NS CD sensor due to the inner filter effect. This was further supported by the fact that with the increasing amount of metanil yellow in the NS CD solution, the characteristic bands of metanil yellow appeared at 273 nm and 438 nm. Their intensity increased with the increase in the concentration of metanil yellow (Fig. S25†).

The fluorescence decay profile of NS CDs in the absence and presence of metanil yellow did not change. However, the lifetime remained almost the same in the absence and presence of metanil yellow (Table S6, Fig. S26†).

From Fig. 6, it is noted that the shape of the emission spectrum changes, and a new fluorescence peak appeared at 510 nm on the addition of a higher concentration of metanil yellow. This could be because metanil yellow as a fluorescence absorber has maximum absorption at 438 nm and has no absorption in 500–600 nm; so a new fluorescence peak of the NS CD/metanil yellow mixture appeared. Such a phenomenon has been cited in the literature for the inner filter effect (Scheme 1).[47,48]

3.7. Real sample assay: identification of metanil yellow in turmeric powder

To check the real-time application of the prepared N and S co-doped CDs as a selective and sensitive fluorescent sensor, the CDs was used as a sensor to detect the inedible azo dye metanil yellow in commercially available turmeric powder.

As shown in Fig. S27a,† the fluorescence intensity of the NS CDs decreases on the successive addition of small amounts of turmeric powder solution containing metanil yellow in increasing amounts, respectively. As noted from Fig. S27a,† the fluorescence intensity of the NS CD solution displayed no characteristic change on the addition of the turmeric powder solution aliquot without metanil yellow. Fig. S27b† showed a linear relationship between the fluorescence intensity of the NS CDs and the increasing amount of metanil yellow added to turmeric powder. The obtained results suggested that the recognition of metanil yellow in an actual sample was both qualitative and quantitative. Thus our nanosensor could be applied to determine the adulteration of food samples with metanil yellow.

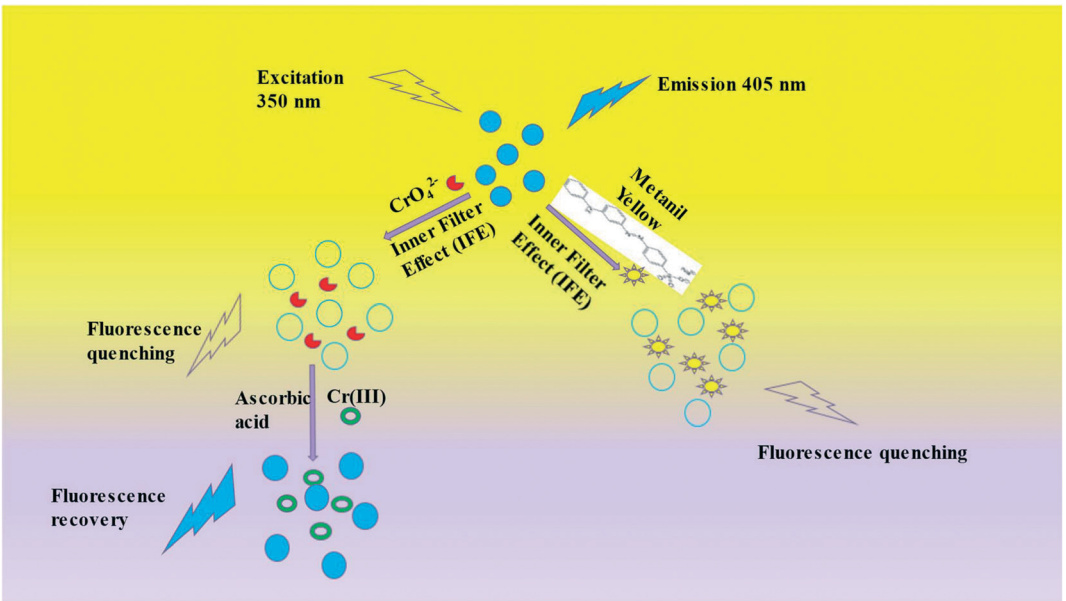

Scheme 1 The schematic representation for the sensing mechanism involved in the presence of Cr(VI), ascorbic acid, and metanil yellow.

4. Conclusion

Successively nitrogen and sulfur co-doped carbon dots as a nanosensor was synthesized by a hydrothermal method using simple carbon, nitrogen, and sulfur sources. The designed nanosensor was productively used for Cr(VI), ascorbic acid, and metanil yellow fluorescence sensing. Relevant techniques adequately characterized the nanosensor. The nanosensor showed promising results in detecting metanil yellow in turmeric powder, thereby paving the way for determining adulteration of food samples with this toxic inedible azo dye.

Author contributions

Ambreen Abbasi: conceptualization, investigation, methodology, formal analysis, writing, and original draft preparation. Mohammad Shakir: supervision.

Conflicts of interest

There are no conflicts to declare.

Acknowledgements

SAIF IIT Madras, SAIF IIT Bombay, and SAIF MIG University are acknowledged for providing Raman, TEM, quantum yield, fluorescence lifetime, and elemental analysis facilities. The chemistry department, AMU, is acknowledged for providing XRD, FT-IR, and TGA facilities.

References

1 H. Ding, J.-S. Wei, P. Zhang, Z.-Y. Zhou, Q.-Y. Gao and H.-M. Xiong, *Small*, 2018, **14**, 1800612.
2 A. Saravanan, M. Maruthapandi, P. Das, S. Ganguly, S. Margel, J. H. T. Luong and A. Gedanken, *ACS Appl. Bio Mater.*, 2020, **3**, 8023–8031.
3 V. Ramanan, S. H. Subray and P. Ramamurthy, *New J. Chem.*, 2018, **42**, 8933–8942.
4 C. S. Estes, A. Y. Gerard, J. D. Godward, S. B. Hayes, S. H. Liles, J. L. Shelton, T. S. Stewart, R. I. Webster and H. F. Webster, *Carbon*, 2019, **142**, 547–557.
5 Y. Wang, S. H. Kim and L. Feng, *Anal. Chim. Acta*, 2015, **890**, 134–142.
6 Y. Dong, H. Pang, H. B. Yang, C. Guo, J. Shao, Y. Chi, C. M. Li and T. Yu, *Angew. Chem., Int. Ed.*, 2013, **52**, 7800–7804.
7 Y. Sun, C. Shen, J. Wang and Y. Lu, *RSC Adv.*, 2015, **5**, 16368–16375.
8 B. B. Chen, M. L. Liu, C. M. Li and C. Z. Huang, *Adv. Colloid Interface Sci.*, 2019, **270**, 165–190.
9 P. Ni, Q. Li, C. Xu, H. Lai, Y. Bai and T. Chen, *Appl. Surf. Sci.*, 2019, **494**, 377–383.
10 Q. Ye, F. Yan, Y. Luo, Y. Wang, X. Zhou and L. Chen, *Spectrochim. Acta, Part A*, 2017, **173**, 854–862.
11 J. Chen, J. Liu, J. Li, L. Xu and Y. Qiao, *J. Colloid Interface Sci.*, 2017, **485**, 167–174.
12 E. F. C. Simões, J. M. M. Leitão and J. C. G. Esteves da Silva, *Anal. Chim. Acta*, 2017, **960**, 117–122.
13 S. Xu, Y. Liu, H. Yang, K. Zhao, J. Li and A. Deng, *Anal. Chim. Acta*, 2017, **964**, 150–160.
14 A. Pal, M. P. Sk and A. Chattopadhyay, *Mater. Adv.*, 2020, **1**, 525–553.
15 A. Pal, G. Natu, K. Ahmad and A. Chattopadhyay, *J. Mater. Chem. A*, 2018, **6**, 4111–4118.
16 K. Chen, W. Qing, W. Hu, M. Lu, Y. Wang and X. Liu, *Spectrochim. Acta, Part A*, 2019, **213**, 228–234.
17 R. Vaz, J. Bettini, J. G. F. Júnior, E. D. S. Lima, W. G. Botero, J. C. C. Santos and M. A. Schiavon, *J. Photochem. Photobiol., A*, 2017, **346**, 502–511.
18 H. Zhang, Y. Huang, Z. Hu, C. Tong, Z. Zhang and S. Hu, *Microchim. Acta*, 2017, **184**, 1547–1553.
19 H. Laddha, P. Yadav, Y. Jain, M. Sharma, M. Reza, M. Agarwal and R. Gupta, *J. Mol. Liq.*, 2022, **346**, 117088.
20 S. R. Anand, A. Bhati, D. Saini, N. Chauhan, P. Khare and S. K. Sonkar, *ACS Omega*, 2019, **4**(1), 1581–1591.
21 L.-L. Feng, Y.-X. Wu, D.-L. Zhang, X.-X. Hu, J. Zhang, P. Wang, Z.-L. Song, X.-B. Zhang and W. Tan, *Anal. Chem.*, 2017, **89**, 4077–4084.
22 X. Lv, H. Man, L. Dong, J. Huang and X. Wang, *Food Chem.*, 2020, **326**, 126935.
23 X. Tian and Z. Fan, *J. Photochem. Photobiol., A*, 2021, **413**, 113261.
24 R. Heydari and M. R. D. Bazvand, *Food Anal. Methods*, 2019, **12**, 1949–1956.
25 H. Bi, A. C. Fernandes, S. Cardoso and P. Freitas, *Sens. Actuators, B*, 2016, **224**, 668–675.
26 K. Dhara and R. M. Debiprosad, *Anal. Biochem.*, 2019, **586**, 113415.
27 S. Kathiravan, E. Sundaram, B. A. Paulraj, P. M. Johnson, S.-T. Huang, V. Mani and V. S. Vasantha, *Food Chem.*, 2020, **332**, 127150.
28 S. Chandra, D. Bano, P. Pradhan, V. K. Singh, P. K. Yadav, D. Sinha and S. H. Hasan, *Anal. Bioanal. Chem.*, 2020, **412**, 3753–3763.
29 S. Chandra, V. K. Singh, P. K. Yadav, D. Bano, V. Kumar, V. K. Pandey, M. Talat and S. H. Hasan, *Anal. Chim. Acta*, 2019, **1054**, 145–156.
30 D. Bano, V. Kumar, V. K. Singh and S. H. Hasan, *New J. Chem.*, 2018, **42**, 5814–5821.
31 Y. Gao, X. Yan, M. Li, H. Gao, J. Sun, S. Zhu, S. Han, L.-N. Jia, X.-E. Zhao and H. Wang, *Anal. Methods*, 2018, **10**, 611–616.
32 S. Dhakal, K. Chao, W. Schmidt, J. Qin, M. Kim and D. Chan, *Foods*, 2016, **5**, 36.
33 R. Jain, N. Sharma and K. Radhapyari, *European Water*, 2009, **27**, 43–52.
34 A. Pal, A. Bhakat and A. Chattopadhyay, *J. Phys. Chem. C*, 2019, **123**, 19421–19428.
35 Y. Wang, S. Kalytchuk, Y. Zhang, H. Shi, S. V. Kershaw and A. L. Rogach, *J. Phys. Chem. Lett.*, 2014, **5**, 1412–1420.
36 X. Li, S. Zhang, S. A. Kulinich, Y. Liu and H. Zeng, *Sci. Rep.*, 2014, **4**, 4976.

37 P. Das, S. Ganguly, S. Mondal, M. Bose, A. K. Das, S. Banerjee and N. C. Das, *Sens. Actuators, B*, 2018, **266**, 583–593.
38 S. Song, F. Liang, M. Li, F. Du, W. Dong, X. Gong, S. Shuang and C. Dong, *Spectrochim. Acta, Part A*, 2019, **215**, 58–68.
39 W. Liu, C. Li, X. Sun, W. Pan, G. Yu and J. Wang, *Nanotechnology*, 2017, **28**, 485705.
40 H. Yuan, J. Yu, S. Feng and Y. Gong, *RSC Adv.*, 2016, **6**, 15192–15200.
41 Y. Chen, Y. Dong, H. Wu, C. Chen, Y. Chi and G. Chen, *Electrochim. Acta*, 2015, **151**, 552–557.
42 M. Zheng, Z. Xie, D. Qu, D. Li, P. Du, X. Jing and Z. Sun, *ACS Appl. Mater. Interfaces*, 2013, **5**, 13242–13247.
43 S. Huang, H. Qiu, F. Zhu, S. Lu and Q. Xiao, *Microchim. Acta*, 2015, **182**, 1723–1731.
44 K. A. N. Upamali, L. A. Estrada and D. C. Neckers, *Anal. Methods*, 2011, **3**, 2469–2471.
45 G. Zhang, Y. Ma, L. Wang, Y. Zhang and J. Zhou, *Food Chem.*, 2012, **133**, 264–270.
46 V. K. Singh, V. Singh, P. K. Yadav, S. Chandra, D. Bano, V. Kumar, B. Koch, M. Talat and S. H. Hasan, *New J. Chem.*, 2018, **42**, 12990–12997.
47 Y. Hu and Z. Gao, *J. Hazard. Mater.*, 2020, **388**, 122073.
48 D. Zhao, X. Liu, Z. Zhang, R. Zhang, L. Liao, X. Xiao and H. Cheng, *Nanomaterials*, 2019, **9**, 1556.